

Supplementary Information

High-Fidelity ATP Imaging *via* an Isothermal Cascade Catalytic Amplifier

Zhiqiao Zou,^a Min Pan,^b Fengye Mo,^a Qunying Jiang,^a Ailing Feng,^a Yizhuo Zhou,^a

Fuan Wang*^a and Xiaoqing Liu*^a

^aCollege of Chemistry and Molecular Sciences, Wuhan University, Wuhan 430072, P.

R. China.

^bFrontier Science Center for Immunology and Metabolism, Medical Research Institute,

Wuhan University, Wuhan 430072, P.R. China.

*To whom correspondence should be addressed. E-mail: fuanwang@whu.edu.cn

(F.W.); xiaoqingliu@whu.edu.cn (X.L.)

Table of Contents

Experiment Section	S2
Table S1. Oligonucleotide sequences of the study	S7
Figure S1. Illustration of different CHA-DNAzyme systems	S8
Figure S2. Fluorescence assay of ATP <i>in vitro</i>	S9
Figure S3. Illustration of the single-staged CHA amplifier.....	S10
Figure S4. Illustration of the single-staged DNAzyme amplifier	S11
Figure S5. Characterization of MnO ₂ NP	S12
Figure S6. Monitoring the adsorption of Cy5-DNA on MnO ₂ NP.....	S13
Figure S7. Characterization of MnCD.....	S14
Figure S8. Stability analysis of MnCD.....	S15
Figure S9. Nuclease resistance of MnCD.....	S16
Figure S10. GSH-stimulated exposure of DNA nanoprobe	S17
Figure S11. Mn ²⁺ -dependent DNAzyme biocatalysis	S18
Figure S12. Flow cytometry analysis of intracellular MnCD uptake	S19
Figure S13. Impact of GSH or ATP regulators on intracellular ATP imaging	S20
Figure S14. CLSM imaging of endogenous ATP in different cells.....	S21
Figure S15. The biocompatibility of MnCD.....	S22
Figure S16. Time-dependent fluorescence images of tumor-bearing mice	S23
Figure S17. <i>Ex vivo</i> fluorescence images of tumor and major organs of mice.....	S24
References	S25

Experimental Section

Materials. All HPLC-purified oligonucleotide sequences except Chlorin e6-labeled S_3 were synthesized by Sangon Biotech. Co., Ltd. (Shanghai, China). Chlorin e6-labeled S_3 was synthesized by Takara Biotech Co., Ltd. (Dalian, China). Penicillin-streptomycin, 4-(2-Hydroxyethyl) piperazine-1-ethanesulfonic acid sodium salt (HEPES), sodium chloride, magnesium chloride, adenosine 5'-triphosphate disodium salt hydrate (ATP) and glutathione (GSH) were purchased from Sigma-Aldrich (MO, USA). RNase-Free Deionized Water was purchased from TIANGEN Biotech Co., Ltd. (Beijing, China). Tris/Borate/EDTA (TBE) buffer, GelRed, were purchased from Bio-Rad (USA). Potassium permanganate ($KMnO_4$) and dimethyl sulfoxide (DMSO) were purchased from Sinopharm Chemical Reagent Co., Ltd. (Shanghai, China). 4,6-Diamidino-2-phenylindole (DAPI), 2',7'-dichlorofluorescein diacetate (DCFH-DA), 3-(4,5-Dimethyl-2-thiazolyl)-2,5-diphenyl-2-H-tetrazolium bromide (MTT) and annexin V-FITC/PI cell apoptosis kit were purchased from Beyotime Biotech. Co., Ltd. (Shanghai, China). Dulbecco's modified Eagle's medium (DMEM), fetal bovine serum (FBS), trypsin, Dulbecco's phosphate buffered saline (PBS) were purchased from GIBCO Invitrogen Corp. N-Ethylmaleimide (NEM), N-Acetyl-L-Cysteine (NAC) and oleic acid (OA) were purchased from Aladdin Reagent Co., Ltd (Shanghai, China). 4T1 cells were obtained from the Shanghai Institutes for Biological Sciences (SIBS). Ultrapure water used throughout the study was obtained by using a Milli-Q apparatus (Millipore, Bedford, MA).

Apparatus. Morphology of the nanoparticle was imaged by scanning electron microscopy (Zeiss Merlin Compact, Germany) and transmission electron microscopy (HT-7700, Hitachi, Japan). The element composition of the nanoparticle was analyzed by energy dispersive spectroscopy (Zeiss Merlin Compact, Germany). Zeta potential and dynamic light scattering analysis were carried out on Zetasizer (NanoZS90, Malvern, UK). The gel was imaged by FluorChem FC3 (Protein Simple, San Jose, CA) under UV ($\lambda = 365$ nm) irradiation. Fluorescent spectra were measured by fluorescence

spectrophotometer (Cary eclipse, Agilent Technologies, USA). UV-Vis absorption spectra were recorded by a UV-2600 Shimadzu spectroscope. Cell viability was measured using Multiskan GO (Thermo Scientific). Flow cytometry analysis was conducted by flow cytometer (Beckman Coulter Cyto-FLEX™ (CytoFLEXS)). All cellular fluorescence images were collected with Leica TCS-SP8 laser scanning confocal microscopy system. Mice imaging was performed with an IVIS Imaging System.

Preparation of MnO₂ nanoparticle. For the synthesis of MnO₂ nanoparticle,¹ 0.1 g of KMnO₄ was dissolved in 50 mL of deionized water, and the mixture was fleetly stirred for about 30 min. A total of 1.0 mL of OA was then added. The resulting mixture was reacted for 5 h. The crude brown-black product was washed several times with water and methanol to remove any possible residual reactants. To estimate the concentration of MnO₂ nanoparticle, 4.0 mL of stock solution was dried in a drying oven at 70 °C and weighed.

Preparation of MnCD. In order to implement the physisorption of DNA amplifier on MnO₂ nanoparticle, the DNA amplifier was incubated with MnO₂ nanoparticle at the desired concentration for 20 min at room temperature.² Then the HEPES buffer (10 mM, pH 7.2, 2 mM MgCl₂ and 150 mM NaCl) was added and incubated for 20 minutes at room temperature. Finally, the mixture was centrifuged to obtain the final product.

Native polyacrylamide gel electrophoresis. The 12% polyacrylamide gel electrophoresis required in the experiment was prepared using 1×TBE buffer (89 mM Tris, 89 mM boric acid, 2.0 mM EDTA, pH 8.3). Then 10 μL samples were mixed with 2 μL 6×loading buffer and loaded into gaps of freshly prepared 12% polyacrylamide gel. Electrophoresis was performed at 110 V in 1×TBE buffer (89 mM Tris, 89 mM boric acid, 2.0 mM EDTA, pH 8.3) for 1.5 h. After staining in diluted GelRed solution for 15 min, the gel was imaged by FluorChem FC3 (Protein Simple, San Jose, CA) under UV ($\lambda = 365$ nm) irradiation.

Fluorescence assay. The DNA strand **A** was incubated with DNA strand **B** for 2 h at

37 °C before developing a follow-up reaction. All fluorescence experiments were carried out in reaction buffer (10 mM HEPES, pH 7.2, 100 mM NaCl), and the reaction mixtures were incubated at 37 °C for 5 h. The concentrations of **A** and **B** strands were fixed at 75 nM. The concentrations of hairpins were 400 nM, and the concentration of substrate **S** was 800 nM unless specifically indicated. The fluorescence spectra were collected from 650 to 740 nm upon exciting the samples at 640 nm.

Cell culture. Unless specifically indicated, 4T1 cells were cultured in DMEM supplemented with 10% fetal bovine serum and 1% penicillin-streptomycin at 37 °C in a humid atmosphere with 5% CO₂ and 95% air.

***In vitro* cellular uptake.** 4T1 cells were seeded in a 12-well plate (1×10^5 cells per well) overnight. Then these cells were incubated with MnCD (10 µg/mL) for different times (1 h, 2 h, 4 h, 6 h, 8 h or 10 h). In addition, the untreated 4T1 cells served as a control. After the specified time, the cells were washed with PBS for three times. Finally, the cells were digested by 0.25%-trypsin-EDTA and prepared to flow cytometry analysis immediately.

Intracellular ATP imaging. Concisely, 4T1 cells were seeded in confocal dishes at a density of 1.5×10^5 cells each dish for overnight. The cells were incubated with different DNA nanoprobes for 12 h. Then, the 4T1 cells were washed with PBS. After the cells were fixed with paraformaldehyde, the nuclei were labeled with DAPI. The fluorescence images were observed by Leica TCS-SP8 laser scanning confocal microscopy system. The excitation wavelength was 640 nm and the emission was collected between 650 and 720 nm.

Measurement of ROS generation. The intracellular ¹O₂ expression was studied using reactive oxygen species assay kit. Concisely, 4T1 cells were seeded in a 12-well plate (2.5×10^5 cells per well) overnight, and then incubated with different materials for 10 h. After removing different materials, the cells were washed three times with PBS. 4T1 cells alone were used as a control. Then, DCFH-DA (5 µM) in the DMEM without

FBS was incubated with the cells in a cell incubator for 30 min and washed three times with PBS. After that, the wells were exposed to irradiation with a 660 nm laser (0.2 W cm^{-2}) for 5 min. Finally, the cells were collected, centrifuged and resuspended in PBS. The expression level of intracellular $^1\text{O}_2$ expression was analyzed by flow cytometer. In addition, the intracellular $^1\text{O}_2$ expression can be monitored by Cytation™ 5 Cell Imaging Multi-Mode. Similarly, 4T1 cells were seeded in a 12-well plate (2.5×10^5 cells per well) overnight. After treated with different materials for 10 h, the cells were washed three times with PBS. Then, the 4T1 cells were incubated with DCFH-DA ($5 \mu\text{M}$) in the DMEM without FBS for 30 min and washed three times with PBS. The cells were exposed to the 660 nm laser for 10 min. Finally, Cytation™5 Cell Imaging multi-mode was used to rapidly analyze the intracellular $^1\text{O}_2$ expression level.

Cytotoxicity assay. Cell viability was tested *via* MTT (3-(4,5-dimethylthiazol-2-yl)-2,5-diphenyltetrazolium bromide) assay. Before adding different materials, 4T1 cells were seeded in a 96-well plate (3×10^4 cells per well) overnight. To investigate the biocompatibility of MnCD, different concentrations of MnCD were added into each well of 96-well plates, and the cells were continued to be cultured for 12 h. After the MnCD of different concentrations were sucked out of the 96-well plate, the cells were washed twice with PBS. Then, $100 \mu\text{L}$ of 0.5 mg/mL of MTT stock solution in PBS was added into every plate and incubated for another 4 h. After removing the MTT, the $150 \mu\text{L}$ dimethyl sulfoxide (DMSO) was added to dissolve the formazan. The absorbance at 490 nm was recorded using the microplate reader. The untreated cells were used as the blank group. The cell viability was calculated by the ratio of the absorbance of blank group. To investigate of the photodynamic therapeutic efficiency *in vitro*, the cells were treated with different nanoprobes for 12 h and then exposed to the 660 nm laser for 5 min. After 24 h, the cell viability was detected by MTT assay.

Apoptosis assay by annexin V-FITC/PI staining. Apoptosis rates were studied using dead cell apoptosis kit with Annexin V-FITC and PI (Thermal Fisher Scientific). 4T1

cells were seeded in a 6-well plate (1.5×10^5 cells per well) overnight, and then were incubated with different materials for 10 h followed by irradiation for 10 min. After 12 h, the cells were washed with PBS for three times. Then the cells were harvested with 0.25% trypsin solution without EDTA. After centrifugated at 1500 rpm for 5 min, the cells were incubated with 500 μ L $1 \times$ binding buffer containing 5 μ L of annexin V-FITC for 15 min and 10 μ L of PI for 5 min at 4 °C in the dark. Finally, the 4T1 cells were subjected to flow cytometry.

Hemolysis test. Firstly, the blood samples were taken using standard ophthalmic vein sampling techniques. Then, the blood samples were purified to resuspend in 10 mL PBS immediately. After that, different concentrations of MnCD were incubated with red blood cells (RBCs) solution for 30 min at 37 °C. In addition, water and PBS were incubated with RBCs and used as positive and negative controls. Then, the supernatant was obtained by centrifugation at 10000 rpm for 5 min. The hemolysis was calculated using the following formula: Hemolysis (%) = $100 \times (\text{sample absorbance} - \text{negative control absorbance}) / (\text{positive control absorbance} - \text{negative control absorbance})$.

***In vivo* fluorescence imaging.** All animal experiments were carried out according to the Principles of Laboratory Animal Care (People's Republic of China). The animal protocol was under the approval of the Laboratory Animal Welfare and Ethics Committee Training Practitioner Institute of Hubei Province (AUP number: WP20210446). 2×10^6 4T1 cells were subcutaneously injected into BALB/c female nude mice (4–6 weeks old, ~20 g) to establish a tumor-bearing mice model. Tumor volume was analyzed by this formula: $V = (L \times W^2)/2$ (L, the longest diameter and W, the shortest diameter). 4T1-bearing mice with tumor volume of about 100 mm³ were randomly divided into 3 groups and respectively treated with MnCD, MnC, CMnCD (4 mg/kg) *via* intratumoral injection. Fluorescence images of live mice were collected with an IVIS imaging system. To confirm the *in vivo* distribution of nanoprobe, mice were sacrificed 16 h post-injection. The main organs (liver, heart, lung, spleen, tumor and kidneys) were collected for *ex vivo* imaging.

Table S1. The DNA sequences used in this work.

Name	Sequence (5'→3')
A	5'-TGG AAA CAC CAC CCA TAT CGC T ACC TGG GGG AGT ATT GCG GAG GAA GGT-3'
B	5'-CCC AGG TAG CGA TAT-3'
H₁	5'-GTC ATT CAG CGA TAT GGG TGG TGT TTC CAC CCA TGT ACG AAA CAC CAC CCA TGT ACA GTC A-3'
H_{1F}(Cy5)	5'-Cy5-GTC ATT CAG CGA TAT GGG TGG TGT TTC CAC CCA TGT ACG AAA CAC CAC CCA TGT ACA GTC A -3'
H_{1F}(Cy5+BHQ-2)	5'-Cy5-GTC ATT CAG CGA TAT GGG TGG TGT TTC CAC CCA TGT ACG AAA CAC CAC CCA TGT ACA GTC A-BHQ2-3'
H_{1T}	5'-TTT TTT CAG CGA TAT GGG TGG TGT TTC CAC CCA TGT ACG AAA CAC CAC CCA TGT ACA GTC A-3'
H₂	5'-GTC ATT CAG CGA TGT GTT TCG TAC ATG GGT GGA AAC ACC ACC CAT CAC CCA TGT ACA GTC A-3'
H_{2T}	5'-TTT TTT CAG CGA TGT GTT TCG TAC ATG GGT GGA AAC ACC ACC CAT CAC CCA TGT ACA GTC A-3'
S₁	5'-Cy5-ATTG ACT GTT rA GGA ATG ACT A-BHQ2-3'
S₂	5'-BHQ2-ATTG ACT GTT rA GGA ATG ACT A-Ce6-3'
E₆	5'-GTC ATT CAG CGA TCC GGA ACG GCA CCC ATG TAC AGT CA-3'

We replaced part of DNAzyme sequence in \mathbf{H}_1 or \mathbf{H}_2 hairpin with poly-T sequence and named it \mathbf{H}_{1T} or \mathbf{H}_{2T} . In the presence of ATP, each \mathbf{H}_{1T} - \mathbf{H}_2 or \mathbf{H}_1 - \mathbf{H}_{2T} hybridization band produced only one DNAzyme unit. In addition, the \mathbf{H}_{1T} - \mathbf{H}_{2T} hybridization band could not form effective DNAzyme unit, so it could not recognize and cleave the substrate to produce fluorescence signal. Combined with fluorescence measurements in Fig. 1C, the feasibility of CHA-activated DNAzyme biocatalysts was verified.

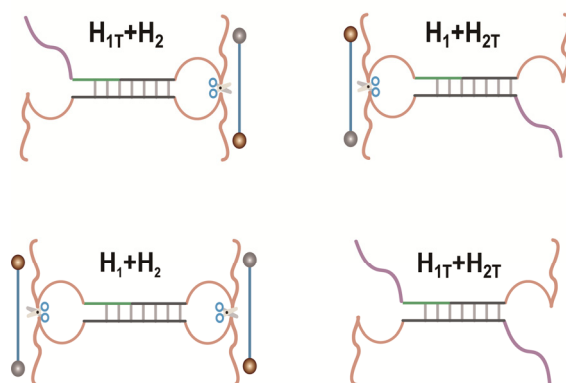


Fig. S1 Illustration for CHA-generated complex of the original cascade amplifier and the \mathbf{H}_{1T} - or/and \mathbf{H}_{2T} -replaced CHA-DNAzyme amplifiers.

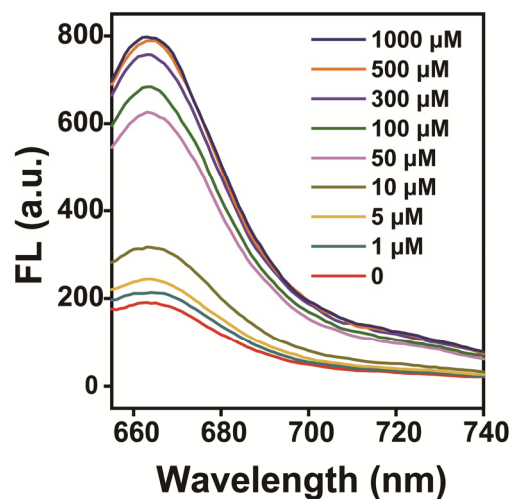


Fig. S2 Fluorescence spectra of the cascade amplifier upon analyzing different concentrations of ATP. The cascade amplifier consisting of 75 nM **A/B**, 400 nM **H₁**, 400 nM **H₂** and 800 nM **S** was reacted at 37 °C in HEPES buffer (10 mM HEPES, 100 mM NaCl, pH 7.2) for a fixed time interval of 5 h.

The CHA amplifier is composed of a partially hybridized duplex (**A/B**), two functional hairpins (**H_{1F}** and **H₂**). The functional hairpin **H_{1F}** is labeled at its 5'- and 3'-ends with a fluorophore/quencher (F/Q) pair. With the addition of ATP, **H_{1F}** and **H₂** are successively opened *via* a toehold-mediated strand displacement, followed by a fluorescence signal from the opened **H_{1F}** hairpin.

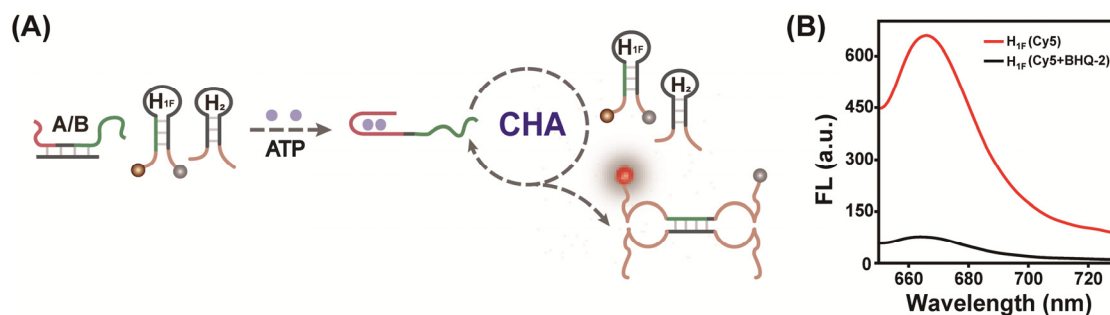


Fig. S3 (A) Illustration of CHA single-stage amplifier. (B) Fluorescence exploration of the differently modified **H_{1F}** (200 nM). Here the **H_{1F}(Cy5)** was only modified with Cy5 at its 5'-end while the **H_{1F}(Cy5+BHQ-2)** was modified at its 5'- and 3'-end with Cy5 and BHQ-2, respectively.

The DNAzyme amplifier consists of E6 DNAzyme and substrate (S) labeled with a fluorophore/quencher (F/Q) pair. In the presence of Mn^{2+} , the activated E6 DNAzyme cleaves S, resulting in fluorescence recovery.

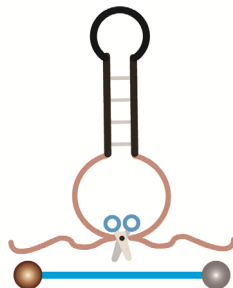


Fig. S4 Illustration of DNAzyme single-stage amplifier.

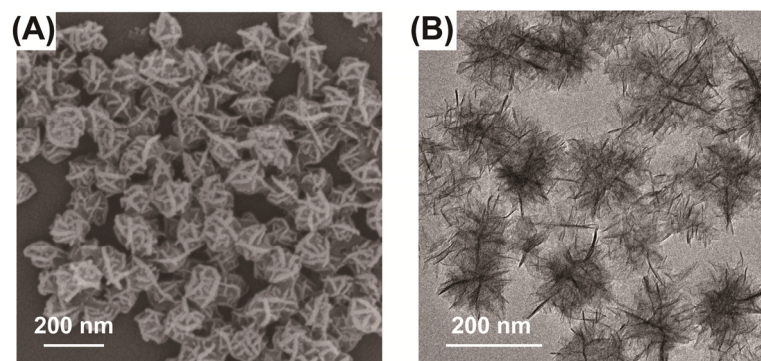


Fig. S5 (A) Scanning electron microscopy (SEM) and (B) transmission electron microscopy (TEM) image of MnO₂ NP.

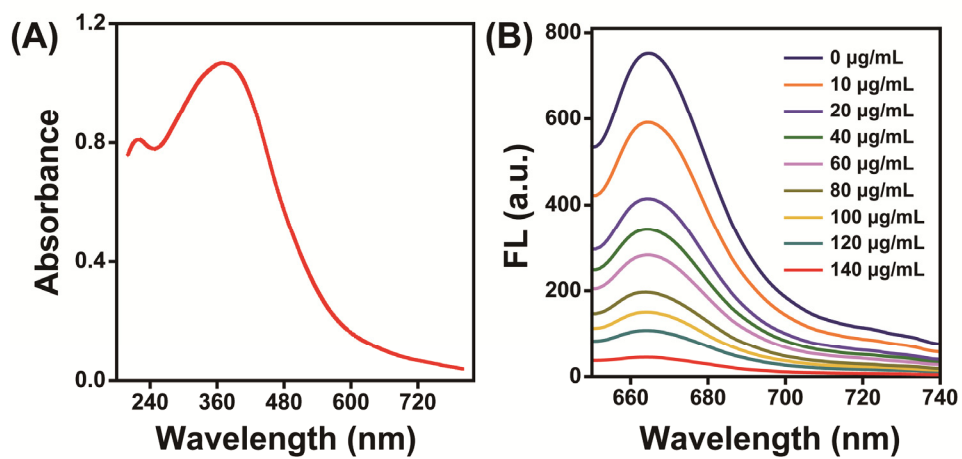


Fig. S6 (A) UV-Vis absorption spectrum of MnO₂ NP. (B) Fluorescence monitoring the adsorption of 400 nM Cy5-labeled DNA that was titrated with MnO₂ NP of different amounts.

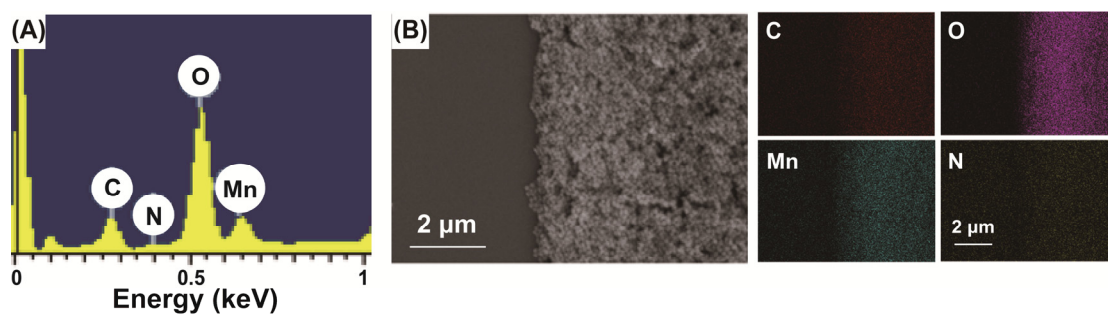


Fig. S7 (A, B) EDX (A) and corresponding elemental mapping (B) of MnCD.

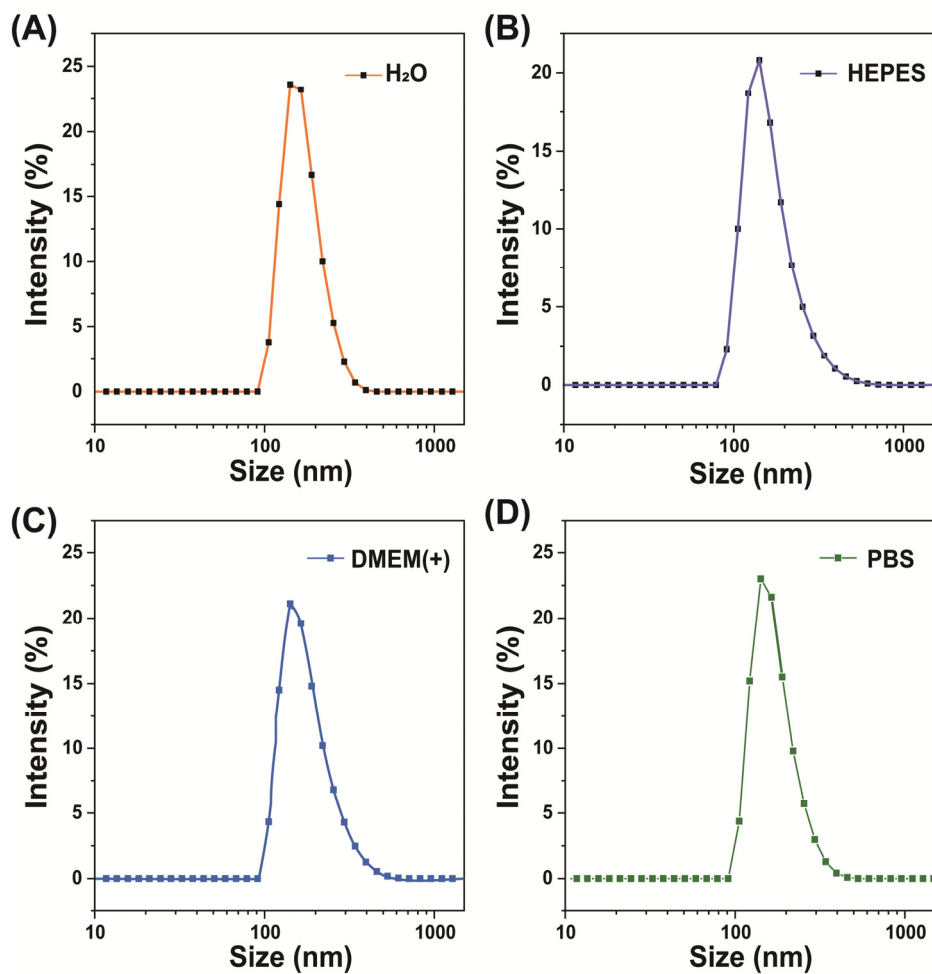


Fig. S8 Hydrodynamic size of MnCD in water (A), HEPES (B), DMEM containing 10% FBS (C), and PBS (D) for 24 h.

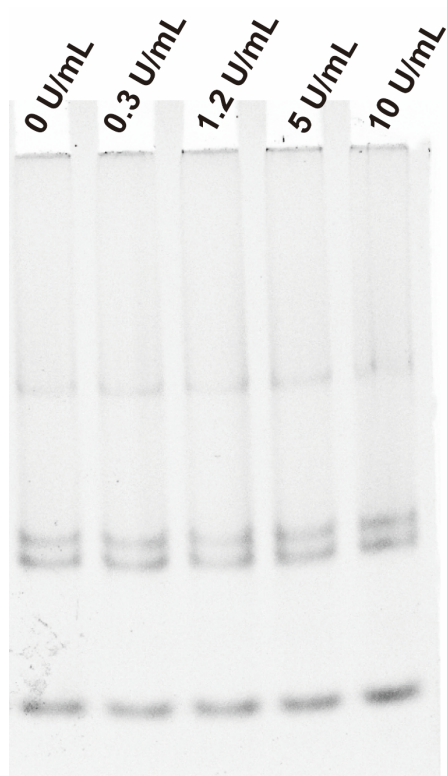


Fig. S9 Gel electrophoresis analysis of MnCD hybrid probe that was treated with DNase I of different concentrations for 24 h.

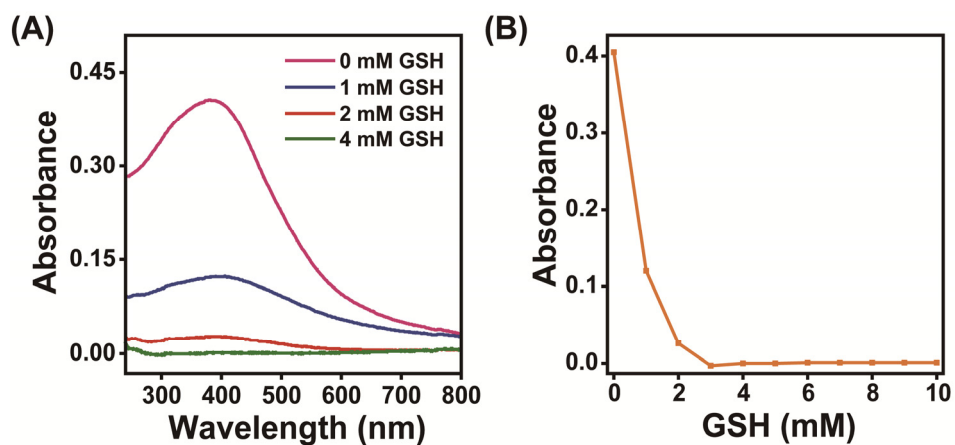


Fig. S10 (A) Degradation of MnO₂ NP under different GSH levels. (B) UV-Vis absorption of MnO₂ NP (at $\lambda=380$ nm) that was treated with GSH of different concentrations. According to the chemical reaction: $\text{MnO}_2 + 2\text{GSH} + 2\text{H}^+ \rightarrow \text{Mn}^{2+} + \text{GSSG} + 2\text{H}_2\text{O}$. MnO₂ NP could be gradually degraded with increasing amounts of GSH.

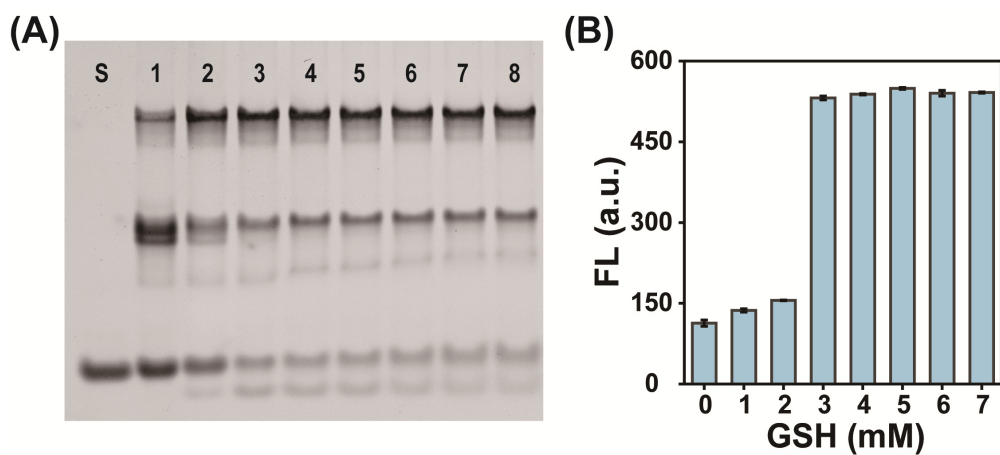


Fig. S11 (A) Gel electrophoresis analysis of the 500 μM ATP-triggered MnCD (100 $\mu\text{g}/\text{mL}$) with GSH of different concentrations (from lane 1 to lane 8: 0 mM, 1 mM, 2 mM, 3 mM, 4 mM, 5 mM, 6 mM, 7 mM). The MnCD was reacted at 37 $^{\circ}\text{C}$ in HEPES buffer (10 mM HEPES, 100 mM NaCl, pH 7.2) for a fixed time interval of 5 h. (B) Fluorescence analysis of the 100 $\mu\text{g}/\text{mL}$ MnO₂ NP-anchored DNA-tethered Cy5 (200 nM) after their incubation with different concentrations of GSH.

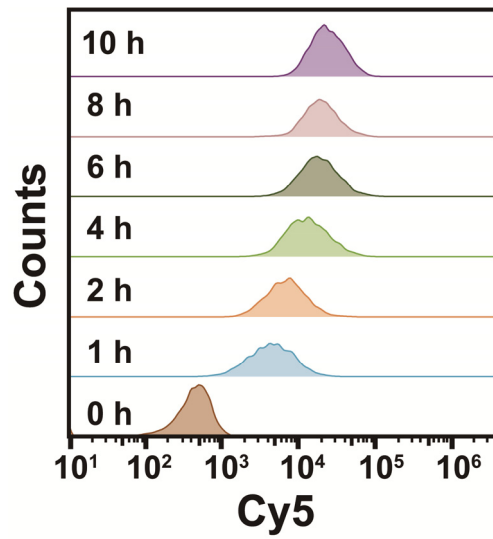


Fig. S12 Optimization of incubation time of MnCD in 4T1 cells. Flow cytometry analysis was acquired by incubating with cells for different time-intervals at 37 °C.

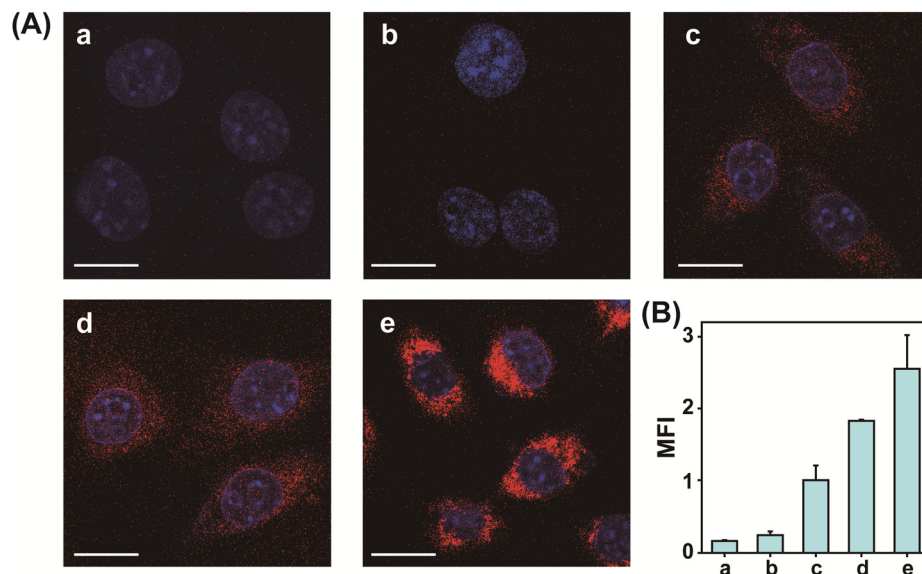


Fig. S13 (A) The MnCD-mediated amplified ATP imaging system in 4T1 cells with different GSH and ATP expressions: (a) pretreatment with 10 μL NEM plus 4 $^{\circ}\text{C}$ (GSH and ATP downregulation), (b) pretreatment with 10 μL NEM (GSH downregulation), (c) intact cells, (d) pretreatment with 100 μL NAC (GSH upregulation) and (e) pretreatment with 100 μL NAC plus 10 mM Ca^{2+} (GSH and ATP upregulation). Scale bar: 10 μm . The cell nuclei were stained with DAPI (blue). (B) Statistical histogram analysis of the fluorescence intensity of these differently treated cells samples. Data are represented as mean \pm SD (n = 3).

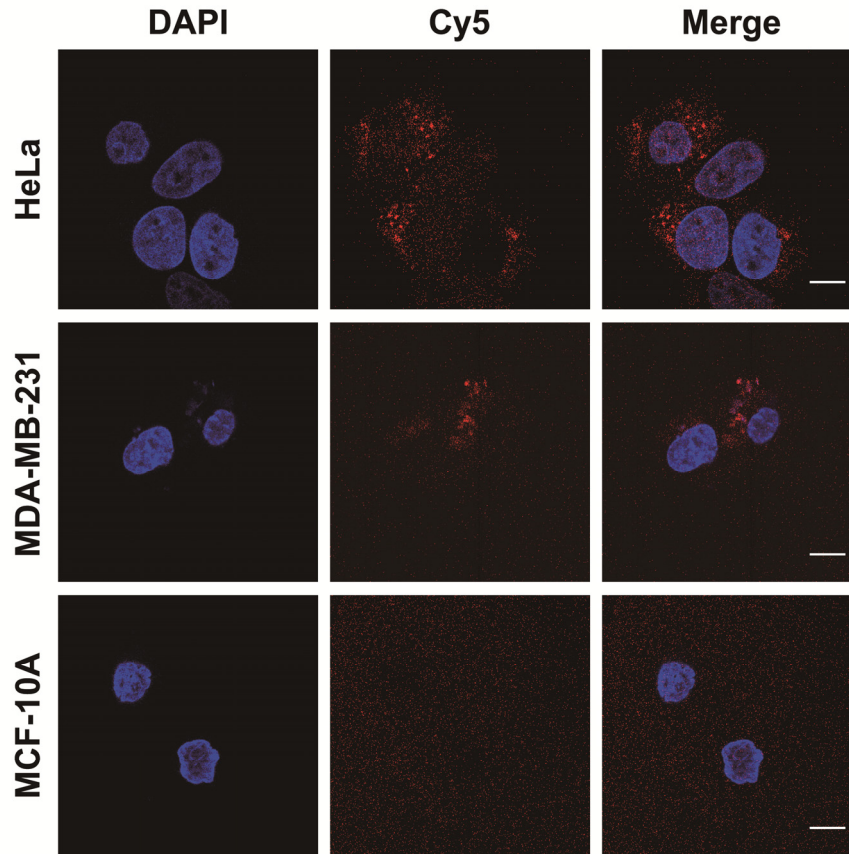


Fig. S14 High-fidelity intracellular ATP imaging in tumor cells (HeLa and MDA-MB-231) and normal cells (MCF-10A) through the MnCD. Scale bar: 10 μm . The cell nuclei were stained with DAPI (blue).

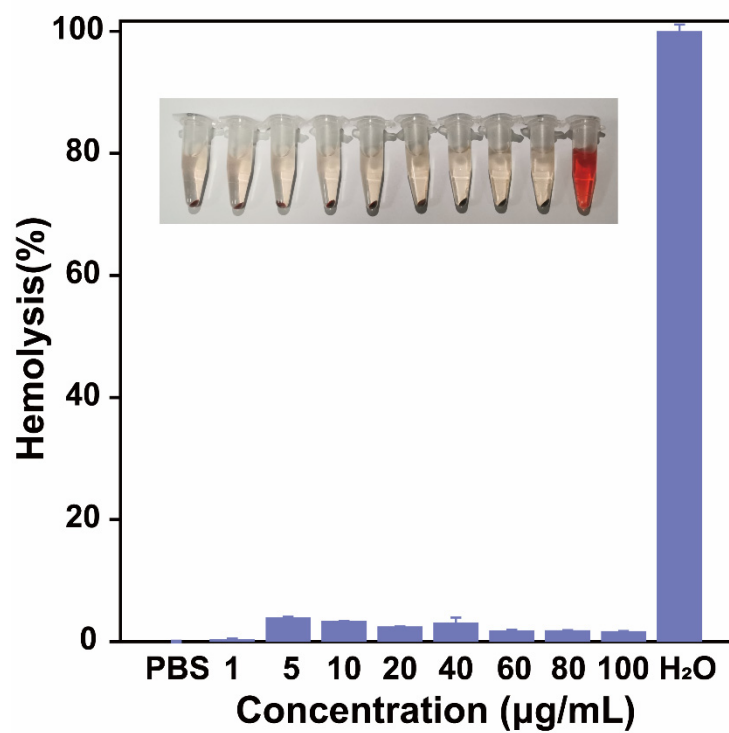


Fig. S15 Hemolysis test of MnCD. PBS and H₂O were used as negative and positive controls, respectively. Error bars denote mean \pm S.D. (n=3).

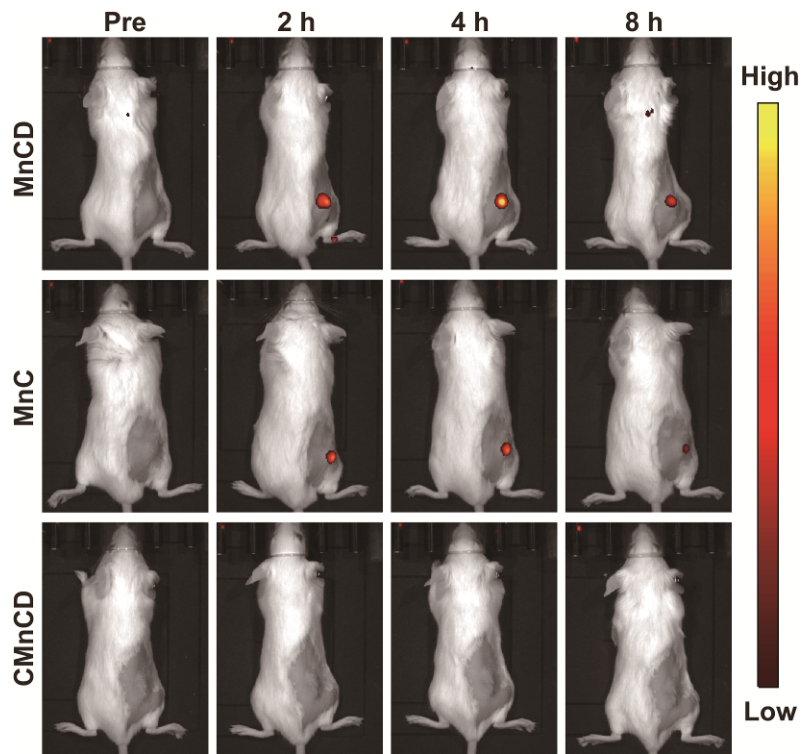


Fig. S16 Whole-body fluorescence imaging of 4T1 tumor-bearing mice at representative time points after intratumoral injection with MnCD, MnC or CMnCD.

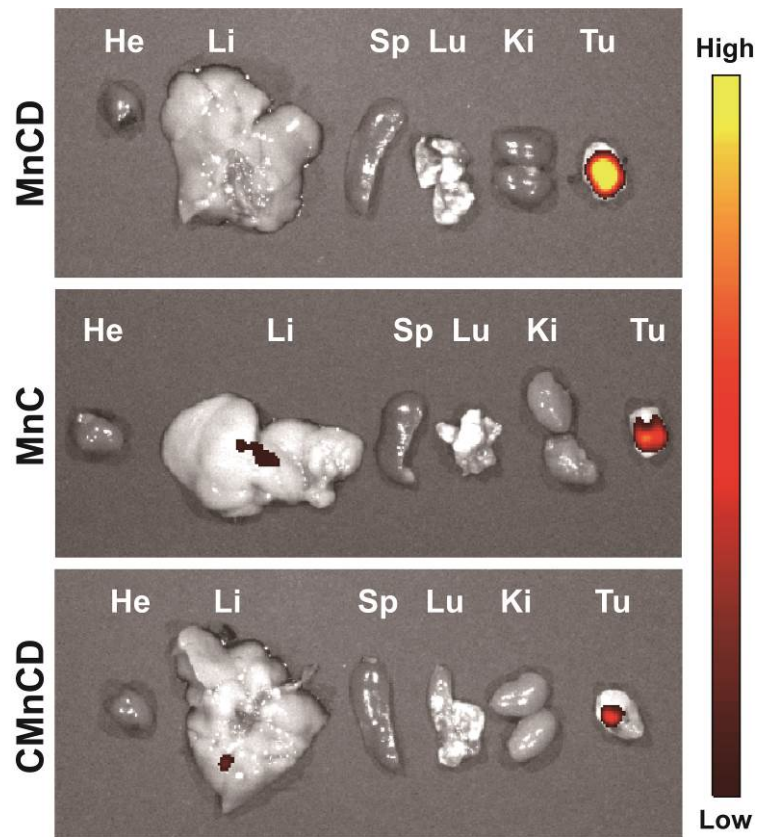


Fig. S17 *Ex vivo* imaging of the major organs and tumor of 4T1 tumor-bearing mice 16 h after intratumoral administration. (He= heart; Li= liver; Sp= spleen; Lu= lung; Ki= kidney; Tu= tumor).

References

- [1]. D. He, L. Hai, X. He, X. Yang and H. Li, *Adv. Funct. Mater.*, 2017, **27**, 1704089
- [2]. J. Wei, H. Wang, Q. Wu, X. Gong, K. Ma, X. Liu and F. Wang, *Angew. Chem., Int. Ed.*, 2020, **59**, 5965-5971.